


This item was submitted to Loughborough's Institutional Repository by the author and is made available under the following Creative Commons Licence conditions.



**CC creative commons**  
COMMONS DEED

**Attribution-NonCommercial-NoDerivs 2.5**

**You are free:**

- to copy, distribute, display, and perform the work

**Under the following conditions:**

**BY:** **Attribution.** You must attribute the work in the manner specified by the author or licensor.


**Noncommercial.** You may not use this work for commercial purposes.

**No Derivative Works.** You may not alter, transform, or build upon this work.

- For any reuse or distribution, you must make clear to others the license terms of this work.
- Any of these conditions can be waived if you get permission from the copyright holder.

**Your fair use and other rights are in no way affected by the above.**

This is a human-readable summary of the [Legal Code \(the full license\)](#).

[Disclaimer](#) 

For the full text of this licence, please go to:  
<http://creativecommons.org/licenses/by-nc-nd/2.5/>



**PREPARATION OF HIGH SOLIDS CONTENT NANO ZIRCONIA  
SUSPENSIONS**

Journal:	<i>Journal of the American Ceramic Society</i>
Manuscript ID:	JACERS-23218.R1
Manuscript Type:	Article
Date Submitted by the Author:	30-Aug-2007
Complete List of Authors:	Santacruz, Isabel; Loughborough University, IPTME; Consejo Superior de Investigaciones Cientificas, Instituto de Ceramica y Vidrio Annapoorani, Ketharam; Loughborough University, IPTME Binner, Jon; Loughborough University, IPTME
Keywords:	colloids, nanomaterials, processing, rheology/rheometry, zirconia: yttria stabilized



## PREPARATION OF HIGH SOLIDS CONTENT NANO ZIRCONIA SUSPENSIONS

Isabel Santacruz<sup>\*†</sup>, Ketharam Anapoorani, Jon Binner<sup>‡</sup>

IPTME, Loughborough University, Loughborough, LE11 3TU Leicestershire, UK

### Abstract

A new colloidal route leading to the production of ~99% dense 3 mol% yttria stabilized zirconia nanostructured ceramics, whilst retaining a final average grain size of ~75 nm, has been developed. The process was based on the production of stable, homogeneous nanosuspensions with solids contents of up to 28 vol% (70 wt%) but viscosities less than 0.05 Pa s at any shear rate in the range of study were obtained. The suspensions were formed by the concentration and optimization of precursor, dilute (5.0 vol%) commercial nanosuspensions, the approach requiring a change of pH, from the 2.4 of the as-received suspension to 11.5, and the use of an appropriate anionic dispersant. Exposure of the nanosuspensions to ultrasound also helped to reduce the viscosity further, though it only worked when the dispersant was optimized. The nanosuspension was slip cast to form homogenous green bodies with densities of ~55% of theoretical without agglomeration in the nanostructure; these were subsequently densified using a two-step sintering technique.

---

\* Author to whom correspondence should be addressed. e-mail: [cruz@icv.csic.es](mailto:cruz@icv.csic.es)

† Currently at the Instituto de Cerámica y Vidrio (CSIC), Madrid, Spain

‡ Member, American Ceramic Society.

Supported by Rolls Royce Fuel Cell Systems Ltd., the PowdermatriX Faraday and the Engineering and Physical Science Research Council (EPSRC), UK, under grant No. GR/S84477/01 and the Spanish Education and Science Ministry under postdoctoral grant No. EX2004-1012.

## I. Introduction

The recent interest in nanocrystalline materials arises from their potential to display unusual properties, including higher hardness and strength in both metals and ceramics,<sup>1,2</sup> and also lower sintering temperatures, offering the ability to save energy and allowing metals and ceramics to be co-fired to a greater extent. If powders can be consolidated into fully dense engineering parts without losing the nanostructure, there is the potential to use the materials for structural, thermal, magnetic, electric or electronic applications such as capacitors, varistors, electronic substrates, wear, thermal barrier and net shape parts, magnets and tools.<sup>2</sup> Conventional, submicron zirconia ceramics are widely used for their excellent mechanical<sup>3</sup> and electrical properties<sup>4</sup> and hence there is considerable interest in investigating the properties of nanostructured yttria stabilized zirconia (YSZ) ceramics.

Commercial nanopowders can now be produced in relatively large quantities, although to date they are generally strongly agglomerated and/or show large amounts of organics derived from their synthesis.<sup>5</sup> However, a major obstacle to the formation of genuinely nanostructured ceramics (average grain size <100 nm) is in the preparation of homogeneous green bodies. Whilst dry forming via die or isostatic pressing is industry's generally preferred route, the strong agglomerates that readily form in dry nanopowders, plus the latter's inability to flow, means that wet forming routes are likely to lead to greater success. Colloidal processing generally allows the production of complex-shaped parts with reduced size and number of pores and higher reliability,<sup>6</sup> however the majority of wet forming routes,<sup>7-11</sup> such as slip casting, in-situ coagulation molding, gel casting and tape casting, require stable slurries with a high solids loading and a low viscosity and this is difficult to achieve with particles in the sub 100 nm range.<sup>12,13</sup> Colloidally stable nanopowder suspensions are known to display a markedly lower

1  
2  
3 volume loading at the same viscosity compared to suspensions with larger particle  
4 sizes.<sup>13</sup>  
5  
6

7  
8 The dispersion of ceramic powders in either an aqueous or a non-aqueous medium  
9 has received considerable attention,<sup>14,15</sup> the nature and strength of the interparticle  
10 forces and also the quantity, shape, and size of the particles determining the rheological  
11 properties of a suspension.<sup>16-18</sup> To achieve adequate distance between the particles in  
12 ceramic suspensions generally requires the use of surfactants that modify the particle  
13 surface. This can be achieved by changing the surface charge, coating the particles with  
14 an organic barrier layer or the combination of the two, i.e. the use of polyelectrolytes,<sup>19-</sup>  
15  
16  
17  
18  
19  
20  
21  
22  
23  
24  
25  
26  
27  
28  
29  
30  
31  
32  
33  
34  
35  
36  
37  
38  
39  
40  
41  
42  
43  
44  
45  
46  
47  
48  
49  
50  
51  
52  
53  
54  
55  
56  
57  
58  
59  
60  
22 although the saturation adsorption and dissociation of the latter in aqueous solution  
are strongly dependent on the pH of the solution.<sup>23,24</sup>

It is known that tetramethylammonium hydroxide (TMAH), tetraethylammonium hydroxide (TEAH) and tetrapropylammonium hydroxide (TPAH) are all quaternary ammonium surfactants for which the positively charged nitrogen atom can be adsorbed onto particle surfaces, enhancing stabilization in some systems<sup>25-28</sup> and also acting as a strong base. The length of the alkyl chain affects the rheology of the suspension, with viscosity, yield stress and thixotropy all increasing with increasing chain length.<sup>27</sup> As a result, the green density decreases as the chain length increases. As a result of these properties, TMAH was studied as basic agent in the present work.

The aim of the present work was to investigate the potential for preparing fully dense, 3 mol% yttria stabilized zirconia nanostructured ceramics whilst retaining a final average grain size of <100 nm. In order to avoid the drawbacks of dry nanopowders, which include uncontrolled agglomeration, the presence of organics (from their synthesis) and potential toxicity due to their ultrafine size, a dilute commercial nano suspension was used to prepare low viscosity, high solid content nanosuspensions.

1  
2  
3 Optimization of the basic agent required to modify the suspension pH, the dispersant  
4 and the use of ultrasound were all performed. The most promising nanosuspensions  
5  
6 were slip cast into green bodies that were subsequently sintered, both the green and  
7  
8 sintered bodies being thoroughly characterized in terms of their density and  
9  
10 nanostructure, the latter in terms of their homogeneity and grain size.  
11  
12  
13  
14  
15  
16  
17  
18  
19  
20

## 21 II. Experimental Procedure

22 The precursor, as-received, nanosuspension (MEL Chemicals Ltd, Manchester, UK)  
23 contained 5.0 vol% of 3 mol% yttria stabilized zirconia nanoparticles (3YSZ) in  
24 deionised water. The solids loading was calculated after drying the suspension in an  
25 oven at 60°C overnight, followed by calcination at 500°C for 2 h. The density of the  
26 dried and calcined powder was measured by He pycnometry (Quantachrome, Fleet,  
27 UK), resulting in values of 4.88 g cm<sup>-3</sup> and 5.55 g cm<sup>-3</sup> respectively. All calculations  
28 were performed with the powder crystallographic density, 6 g cm<sup>-3</sup>.  
29  
30  
31  
32  
33  
34  
35  
36  
37  
38

39 A tetragonal/cubic phase content of 92% was observed in the dried nanopowder  
40 using XRD, the balance being monoclinic. The as-received suspension, which had a pH  
41 of 2.4±0.1, was also characterized in terms of particle size using an AcoustoSizer II  
42 (Colloidal Dynamics, Sydney, Australia) and the dried nanoparticles were examined  
43 using transmission electron microscopy, TEM, (JEOL 2000FX, Jeol, Tokyo, Japan).  
44  
45  
46  
47  
48  
49

50 The effect of both cationic and anionic dispersants were examined. The former,  
51 poly(ethylenimine), PEI, (BDH Chemicals Ltd., Poole, UK), was appropriate for the as-  
52 received acidic suspension,<sup>24</sup> whilst the anionic dispersants required that the pH be  
53 modified to the basic region.<sup>20,23,24</sup> This was achieved using both 35% ammonia solution  
54 (Fisher Scientific, Loughborough, UK) and solid tetramethylammonium hydroxide,  
55  
56  
57  
58  
59  
60

1  
2  
3 TMAH (Aldrich Chemicals Ltd, Dorset, UK), the latter having the advantage of not  
4 involving the initial further dilution of the precursor nanosuspension. When the  
5 ammonia solution was used, the solids content of the nanosuspension fell from 5.0 to  
6 3.3 vol%; with the TMAH, it remained at 5.0 vol% and the suspension displayed  
7 superior stability. Additions of 6.7 wt% of TMAH, as a function of the suspension  
8 solids content, were found to be required to modify the as-received suspension's pH  
9 from 2.4 up to  $11.5 \pm 0.1$ . The anionic dispersants investigated were Dispex A40, an  
10 ammonium polyacrylate-based surfactant,  $\text{NH}_4\text{PAA}$ , (Ciba Speciality Chemicals,  
11 Bradford, UK), and triammonium citrate, TAC, (FSA Laboratory, Loughborough, UK).  
12 The latter was studied because it is a relatively short molecule that was considered to be  
13 less likely to be broken by the application of ultrasound, which was used to break down  
14 any agglomerates present.

15  
16  
17  
18  
19  
20  
21  
22  
23  
24  
25  
26  
27  
28  
29  
30  
31  
32  
33  
34  
35  
36  
37  
38  
39  
40  
41  
42  
43  
44  
45  
46  
47  
48  
49  
50  
51  
52  
53  
54  
55  
56  
57  
58  
59  
60  
The suspensions involving PEI were prepared by mixing 2.0 and 4.0 wt% directly into the as-received suspension; the presence of the strong acid neutralized its basic – $\text{NH}_2$  groups and conferred a positive charge on the polymer skeleton.<sup>19</sup> For the anionic dispersants, 1 to 4.5 wt% additions of Dispex and TAC were introduced to the pH-modified nanosuspension, preliminary work indicating that 2.5 wt% was the optimum addition. The adsorption of dispersants was achieved by shaking the suspensions, on an automatic shaker (KS 260 basic, IKA, Staufen, Germany), in closed plastic bottles for 20 h. Note: in all cases, the amount of the deflocculant addition is expressed in terms of the active matter present in the dispersant with respect to suspension solids loading.

Zeta potential and particle/agglomerate size measurements as a function of pH were performed using an AcoustoSizer II. The as-received suspension was diluted to 1.8 vol% using deionised water due to the difficulties found in performing a continuous titration at higher solids loading in the equipment. Titration was performed from acid to

1  
2  
3 base, using 1M NaOH solution (automatic titration) or by manual addition of TMAH.  
4  
5 Similar measurements were made on the basic diluted suspension (achieved using  
6  
7 ammonia solution) containing 2.5 wt% Dispex A40 or TAC using 1M NaOH and HCl  
8  
9 solutions for pH adjustments.  
10  
11

12  
13 The dilute nanosuspensions were subsequently concentrated in a water bath at 50°C  
14  
15 for between 1 and 4 days, depending on the required final solids loading and, for the  
16  
17 anionically-dispersed suspensions, whether ammonia solution or TMAH was used. For  
18  
19 example, to achieve a solids content of 17 vol% required 4 days for the ammonia  
20  
21 solution-based suspension and only 2 days for that produced using TMAH due to the  
22  
23 higher solids content at the starting point. Throughout the process, the pH was  
24  
25 controlled every two hours, keeping it at  $9.5 \pm 0.1$ , and the suspension was stirred  
26  
27 constantly.  
28  
29

30  
31 As already indicated, in order to break up any agglomerates present, the suspensions  
32  
33 were exposed to ultrasound using a KS150 ultrasound probe (Kerry Ultrasonics Ltd,  
34  
35 Skipton, UK), with an amplitude of 14  $\mu\text{m}$  and a power of 75 W. In all cases, the  
36  
37 ultrasound was applied to 50 ml aliquots of the different nanosuspensions. A variety of  
38  
39 different time periods of ultrasound exposure were investigated, from 0 to 10 minutes.  
40  
41 Note that the ultrasound exposure was performed in 1 minute steps, with the suspension  
42  
43 being stirred at room temperature for 10 minutes between each ultrasound application in  
44  
45 order to avoid excessive heating of the nanosuspension.  
46  
47

48  
49 A “multi-ultrasound” approach was also applied to selected suspensions, as distinct  
50  
51 from the simple ultrasound method described above. The “multi-ultrasound” technique  
52  
53 involved applying ultrasound to the suspension at several different points in the  
54  
55 concentration process until the required solids loading was achieved. For example, the  
56  
57 suspension dispersed with Dispex was exposed to ultrasound 3 times during the  
58  
59  
60



1  
2  
3 evaporation process; 2 minutes at a solids loading of 15 vol%, then a further 5 minutes  
4  
5 when it reached 19 vol% and finally 10 more minutes at 28 vol%. For the TAC-based  
6  
7 suspension, it was found that less ultrasound was required, viz. only two applications, 6  
8  
9 minutes at 24 vol% followed by a further 2 minutes at 28 vol%. In all cases, the  
10  
11 suspensions were held in a cold water bath during ultrasonication the suspension  
12  
13 heating.  
14  
15

16  
17 The size of any agglomerates present in the nanosuspensions was measured using a  
18  
19 Mastersizer 2000 (Malvern Instruments Ltd., Malvern, UK). Based on the results, it is  
20  
21 believed that the agglomerates formed during the evaporation of the suspension were  
22  
23 subsequently broken by the ultrasound, thus allowing more concentrated suspensions to  
24  
25 be prepared. The rheological behavior of the suspensions was determined using a Visco  
26  
27 88 BV viscometer (Bohlin Instruments, Cirencester, UK) with a C30 concentric  
28  
29 cylinder sensor and varying the shear rate from 0 to 1000 s<sup>-1</sup> in 8 minutes without pre-  
30  
31 shearing; the time taken in obtaining the flow curve being distributed equally across the  
32  
33 measurement points. After each exposure to ultrasound, all the suspensions were stirred  
34  
35 for 10 min prior to rheological measurement. To study the effect of ageing on the  
36  
37 agglomerate size and rheology, the suspensions were left for several days in closed  
38  
39 plastic bottles on the shaker before additional measurements were made.  
40  
41  
42  
43  
44

45  
46 To ensure comparisons could be made between the different nanosuspensions, the  
47  
48 agglomerate size and rheological measurements were all made at pH 9.5±0.1 at room  
49  
50 temperature and the viscosity values presented in the results were all taken from the  
51  
52 upward flow curves at a shear rate of 100 s<sup>-1</sup>.  
53  
54

55  
56 The suspensions with the highest solids content whilst retaining a low viscosity were  
57  
58 subsequently slip cast in plaster of Paris moulds to form green bodies measuring 9 mm  
59  
60 diameter by 7 mm thick. The resulting green densities of the bodies formed were

1  
2  
3 measured by the Archimedes' method using mercury. After the removal of the organic  
4 dispersants at 500°C for 2 hours, the green samples were sintered in an electrical  
5 furnace (UAF 16/10, Lenton Thermal Design, Hope Valley, UK) using a two stage  
6 sintering cycle.<sup>29</sup> This involved heating the samples to 1150°C at 20°C min<sup>-1</sup> and  
7 holding them for one minute before the temperature was dropped as rapidly as possible  
8 to 1000°C, where the samples were soaked for 5 or 10 hours. The sintered densities of  
9 the bodies were measured by the Archimedes' method using water.

10  
11  
12  
13  
14  
15  
16  
17  
18  
19  
20 Fracture surfaces of the green and sintered nanozirconia samples were observed by  
21 field emission gun scanning electron microscopy (LEO 1530VP, LEO  
22 Elektronenmikroskopie GmbH, Oberkochen, Germany).

### 23 24 25 26 27 28 29 30 31 32 33 34 35 36 37 38 39 40 41 42 43 44 45 46 47 48 49 50 51 52 53 54 55 56 57 58 59 60

### III. Results and Discussions

The average particle size of the as-received suspension at pH 2.4±0.1 was 16 nm ± 0.5%, which correlated well with the particle size observed using TEM, figure 1.

When PEI was added to the as-received suspension it resulted in an increase in viscosity under all conditions. Table I shows the viscosity of the suspension containing 2.0 wt% PEI, measured at 100 s<sup>-1</sup>, and compares it with the as-received suspension. For this reason, and also because at acidic pH the yttria is dissolved resulting in Y<sup>3+</sup> cations,<sup>30</sup> which would make the processing of concentrated suspensions difficult by promoting coagulation, it was decided to focus on basic pH values.

Figure 2 shows the results of the titration of the 1.8 vol% suspension. Note that since 1 M NaOH was used there was a negligible reduction in solids content with pH change. From the figure it is clear that the isoelectric point (IEP) for the as-received suspension was just below pH 10; this is higher than generally observed in the literature<sup>31,32</sup> and may be due to the presence of residual species, e.g. counter ions, from the preparation of

1  
2  
3 the nanosuspension. At pH values from 2 to 6 the suspension was very stable with a zeta  
4 potential of ~60 mV, however in the basic pH range of 11 to 12, the maximum absolute  
5 value was found to be quite low, ~20 mV. Despite this, the particle size of the 1.8 vol%  
6 suspension at pH 11.5 was 31 nm ( $d_{50}$ ) / 53 nm ( $d_{85}$ )  $\pm 1\%$  suggesting that there were no  
7 significant agglomerates present, even though the zeta potential was low. In the same  
8 figure, the zeta potential curves as a function of pH for the suspensions with 2.5 wt% of  
9 both Dispex and TAC are also shown. It can be seen that the suspensions with these  
10 anionic dispersants had very similar curves with desirably large zeta potential values  
11 over a wide range of pH, from ~8 to 12.  
12  
13  
14  
15  
16  
17  
18  
19  
20  
21  
22  
23  
24

25 Figure 3 reveals that the zeta potential of the as-received nanosuspension changed  
26 smoothly from ~60 mV through to ~-40 mV as the pH was changed from 2.4 to  
27 11.5 $\pm$ 0.1 by the addition of TMAH. The higher absolute value of the zeta potential at  
28 pH 11.5 after the addition of TMAH compared with that obtained by the addition of  
29 NaOH, ~-20 mV, confirms that TMAH provides an extra contribution to stability,  
30 probably related to the adsorption of N+(Me)<sub>4</sub> groups<sup>27</sup> which are not available from  
31 bases such as NaOH. The change in pH resulted in the formation of agglomerates as the  
32 pH passed through the isoelectric point (IEP), which occurred at pH ~9.5 when no  
33 deflocculants were present. Interestingly, the formation of the agglomerates was  
34 reversible and hence no significant agglomeration was observed after crossing the IEP,  
35 figure 3, even though ultrasound was not applied to the suspensions.  
36  
37  
38  
39  
40  
41  
42  
43  
44  
45  
46  
47  
48  
49

50 The flow curves of the nanosuspensions with 2.5 wt% Dispex A40 prepared using  
51 TMAH at a solid content of 19.0 vol% and using ammonia solution at a solid loading of  
52 17.0 vol% are shown in figure 4. In both cases, 2 minutes of ultrasound have been  
53 applied. Both pH agents allowed the formation of moderately concentrated  
54 nanosuspensions with low viscosities, although it may be seen that the use of the  
55  
56  
57  
58  
59  
60

1  
2  
3 TMAH allowed slightly higher concentrations to be achieved whilst retaining a very  
4 similar viscosity. This may be due to 2 reasons: the extra stabilization provided by the  
5 TMAH<sup>27</sup> and/or the longer evaporation time required when ammonia was added due to  
6 the initial suspension dilution, which may contribute to greater agglomeration thus  
7 necessitating longer ultrasound times than were studied in the current work. Whatever  
8 the reason, TMAH was selected as the basic agent for further studies since it avoided  
9 the initial dilution, hence reducing processing time, and yielded a slightly lower  
10 viscosity for a given solids content.  
11  
12  
13  
14  
15  
16  
17  
18  
19  
20  
21

22 The effect of the ultrasound is plotted in figures 5 and 6. These show flow curves for  
23 15.0 vol% solids content dispersed nanosuspensions after 1 and 2 minutes of ultrasound  
24 exposure, figure 5, and flow curves of 19.0 vol% nanosuspensions after 1 to 6 minutes  
25 of ultrasound, figure 6 (a). Dispex A40 was used in both cases. Whilst both curves in  
26 figure 5 displayed shear thinning behavior without thixotropy, the suspension with two  
27 minutes of ultrasound treatment exhibited considerably lower viscosity. A similar  
28 outcome is presented by figure 6, where longer ultrasound times were required with the  
29 higher solids content suspension. Figure 6 (b) shows the viscosity of the 19.0 vol%  
30 suspensions at  $100 \text{ s}^{-1}$  after ultrasound.  
31  
32  
33  
34  
35  
36  
37  
38  
39  
40  
41  
42

43 The stability of the viscosity taken at  $100 \text{ s}^{-1}$  during ageing of a 16.0 vol%  
44 suspension prepared using Dispex A40 after 2, 4 and 8 minutes of ultrasound is shown  
45 in figure 7. Once again, this shows that longer periods of ultrasound exposure result in  
46 more stable suspensions in the range of study, where samples treated for  $\geq 4$  min were  
47 entirely stable for at least 7 days whilst those treated for only 2 min exhibited a fairly  
48 steady increase in viscosity over time. No sedimentation was observed in these  
49 suspensions. Stable suspensions with solids loadings up to 19 vol% could be achieved  
50 with this approach.  
51  
52  
53  
54  
55  
56  
57  
58  
59  
60

1  
2  
3 Figure 8 reveals the effect of ultrasound on the size of the agglomerates present in  
4 the suspension, the  $d_{50}$  value taken from the volume distribution as measured by laser  
5 scattering via a Malvern MasterSizer 2000, as a function of solids content. It can be  
6 seen how the use of ultrasound significantly reduced the size of the agglomerates  
7 present – and also confirms again how at higher solids loadings, longer ultrasound  
8 periods were required.  
9

10  
11 The consequences of the presence of the agglomerates on the microstructure of the  
12 slip cast green samples are illustrated by the fracture surfaces shown in figure 9. Images  
13 (a) and (b) are both from bodies prepared from a 15.0 vol% suspension after 1 and 2  
14 minutes of ultrasound respectively (the samples were prepared from the suspensions  
15 represented in figure 5); it can be seen how the latter is very significantly more  
16 homogeneous since the action of the ultrasound broke up the agglomerates present.  
17 Figures 9 (c) and (d) show the nanostructure obtained by slip casting a 19.0 vol%  
18 suspension after 5 minutes of ultrasound at two different levels of magnification  
19 (prepared from suspensions shown in figure 6). The homogeneity of the structure is  
20 notable.  
21  
22  
23  
24  
25  
26  
27  
28  
29  
30  
31  
32  
33  
34  
35  
36  
37  
38  
39  
40

41 All of the results presented to date were based on the application of ultrasound at the  
42 final solid loading. However, this approach suffered from an upper solid loading limit  
43 beyond which ultrasound could not be applied because the viscosity was too high and  
44 the suspension became a solid even before the application of the ultrasound. This led to  
45 the development of the multi-ultrasound approach described earlier. Figure 10 shows  
46 the results achieved for a 28 vol% suspension when this approach was used. Whilst it  
47 can be seen that a final viscosity of  $<1$  Pa s was achieved even at this high solids content  
48 (28.0 vol%, 70.0 wt%), unfortunately it was discovered that the resulting suspensions,  
49 which were based on Dispex A40, were unstable. They became a gel over time; the  
50  
51  
52  
53  
54  
55  
56  
57  
58  
59  
60

1  
2  
3 higher the solids content achieved, and hence the more ultrasound used, the faster this  
4 occurred. It is believed that excessive use of ultrasound may have damaged the polymer  
5 chain of the dispersant, resulting in an unstable system. This led to the investigation of  
6 tri ammonium citrate, TAC, a shorter chain anionic dispersant, so it is less likely to be  
7 broken by the application of ultrasound, since [the length of the dispersant chain is a key  
8 parameter in the stabilization of nanosuspensions.](#)<sup>33,34</sup>  
9  
10  
11  
12  
13  
14  
15  
16

17 Figure 11 reveals the resulting flow curves for the TAC dispersed suspensions at  
18 different solids loadings and with different exposures to ultrasound; note that the  
19 concentrated suspensions made with TAC exhibited lower viscosities even without the  
20 use of ultrasound than those based on Dispex A40, opening up the potential for  
21 achieving even higher solid content suspensions after optimization. Figure 11 (a) shows  
22 the effect of concentrating the solids loading from the as-received value of 5.0 vol% up  
23 to 24.0 vol% without the use of any ultrasound. [An important increase in the viscosity  
24 and thixotropy may be observed from 9.0 to 24.0 vol% solids loading.](#) Figure 11 (b)  
25 reveals how the viscosity and thixotropy decreased by increasing exposure to ultrasound  
26 from 2 to 6 minutes on a 24.0 vol% nanosuspension. [A great improvement of viscosity  
27 is observed only after 2 minutes of ultrasound, compared with fig. 11 \(a\).](#)  
28  
29  
30  
31  
32  
33  
34  
35  
36  
37  
38  
39  
40  
41  
42

43 Fig. 11 (c) shows the flow curves of two 28.0 vol% suspensions, the first after  
44 application of just 2 min of ultrasound at 24.0 vol% and the second after 2 min of  
45 ultrasound at 24.0 vol% followed by a further 2 min at 28.0 vol%. [When the former  
46 curve is compared with that in fig. 11 \(b\) after 2 min ultrasound, it can be seen how an  
47 increase of just 4 vol% in the solids loading at these high values yields a very  
48 considerable viscosity increase.](#)  
49  
50  
51  
52  
53  
54  
55  
56

57 Table I summarizes the effect of the basic agent and anionic dispersant on the  
58 viscosity (taken at  $100 \text{ s}^{-1}$  from the up-curve) as a function of solids loading with and  
59  
60

1  
2  
3 without the use of ultrasound. The improvement shown by the TMAH / TAC system  
4 over the ammonia solution / Dispex A40 system is clearly visible in terms of the lower  
5 viscosities observed. Fig. 12 shows the viscosity curves of three suspensions in which  
6 TMAH was used as the basic agent. It can be seen that even with the application of a  
7 single, 6 min ultrasound treatment at the end of the concentration process, the use of  
8 TAC results in the 24.0 vol% solids content nanosuspension, fig. 12 (a), having a lower  
9 viscosity than the 19.0 vol% suspension prepared with 2.5 wt% Dispex A40 after the  
10 multi-ultrasound treatment, fig. 12 (b). When the multi-ultrasound process is then  
11 combined with the TAC, 28.0 vol% suspensions can be seen to display a viscosity <0.05  
12 Pa s at all shear rates measured, fig. 12 (c). They were also entirely stable for periods of  
13 at least 15 days, confirming the superiority of TMAH over ammonia solution and TAC  
14 as a dispersant compared to Dispex A40.

15  
16  
17  
18  
19  
20  
21  
22  
23  
24  
25  
26  
27  
28  
29  
30  
31  
32  
33  
34  
35  
36  
37  
38  
39  
40  
41  
42  
43  
44  
45  
46  
47  
48  
49  
50  
51  
52  
53  
54  
55  
56  
57  
58  
59  
60  
These suspensions were slip cast and green density values of ~55% of theoretical  
(6 g cm<sup>-3</sup>) were obtained. Fig. 13 (a) and (b) show the nanostructures of the two-stage  
sintered, slip cast samples prepared from a 19.0 vol% suspension prepared with TMAH  
and Dispex A40 after 5 min of ultrasound; ~99% dense ceramics were obtained with an  
average and uniform grain size of 80 and 90 nm after 5 and 10 h soaking time  
respectively. The equivalent nanostructure for a sample prepared from 28.0 vol%  
suspension made with TAC and the multi-ultrasound treatment after a soaking time of  
10 hours can be seen in fig. 12 (d), its green nanostructure may be seen in fig. 12 (c).  
The sintered sample has an average grain size of 75 nm, i.e. lower than that obtained  
from the equivalent sintering cycle for the sample prepared with Dispex A40, figure 12  
(b), and is much more uniform due to the greater stability and higher solid loading of  
the precursor suspension.

#### IV. Conclusions

A colloidal route has been developed for the production of ~99% dense 3 mol% yttria stabilized zirconia nanoceramics with final average grain sizes of ~75 nm. It is based on the preparation of 3YSZ nanosuspensions with solids contents up to 28.0 vol% but viscosities as low as 0.05 Pa s from commercially available, dilute suspensions. The process is based on a series of steps involving initially adjusting the pH to a value of  $\sim 11.5 \pm 0.1$  from the original value of  $2.4 \pm 0.1$  using (solid) tetramethylammonium hydroxide, TMAH. This is followed by the addition of anionic dispersants. Whilst both Dispex A40, a commercial surfactant based on ammonium polyacrylate, and triammonium citrate, TAC, work, the latter has been found to be more suitable, offering both the potential to achieve lower viscosities at higher solids contents and also more resistance to the subsequent use of ultrasound. The dilute nanosuspensions can then be concentrated by evaporation at 50°C in a water bath. The use of ultrasound energy has been found to be important for breaking any agglomerates that form, thus ensuring that they do not cause a problem in the subsequent nanostructure of the green components formed. Since the higher the solid content of the suspension, the more frequent and the longer periods of ultrasound that were required, an approach based on the use of multiple ultrasound applications for relatively short durations was found to be an appropriate way forward. Whilst this caused problems with nanosuspensions dispersed with Dispex A40, possibly because of damage to the polymer chain, with the shorter chain TAC, high solids content, low viscosity nanosuspensions could be formed that were stable for periods of at least 15 days. This stability range is very high when compared with other nanoparticle suspensions.<sup>35</sup>

Samples produced by slip casting the most promising nanosuspensions could be sintered using a two stage sintering process to yield a final average grain size as fine as



1  
2  
3 ~75 nm. The process by which the nanosuspension was formed is the subject of a patent  
4  
5 application.<sup>36</sup>  
6  
7  
8  
9

## 10 11 12 **Acknowledgements**

13  
14  
15 The authors would like to thank to MEL Chemicals Ltd. for provision of the  
16  
17 precursor nanosuspension free of charge.  
18  
19  
20  
21  
22  
23

## 24 25 **References**

- 26  
27 <sup>1</sup>M. Mayo, "Processing of nanocrystalline ceramics from ultrafine particles," *Int.*  
28  
29 *Mater. Rev.*, **41** [85] 1743-2804 (1996).  
30  
31  
32 <sup>2</sup>M. N. Rittner and T. Abraham, "Economics: Nanostructured Materials: An Overview  
33  
34 and Commercial Analysis," *JOM*, **50** 1160-96 (1998).  
35  
36 <sup>3</sup>J. Kondoh, H. Shiota, K. Kawachi, and T. Nakatani, "Yttria concentration dependence  
37  
38 of tensile strength in yttria-stabilized zirconia," *J. Alloys and Comp.*, **365** 253-58  
39  
40 (2004).  
41  
42 <sup>4</sup>I. Kosacki, T. Suzuki, V. Petrovsky, and H. U. Anderson, "Electrical conductivity of  
43  
44 nanocrystalline ceria and zirconia thin films," *Solid State Ionics*, **136-137** 1225-33  
45  
46 (2000).  
47  
48  
49 <sup>5</sup>I. Santacruz, M I. Nieto, J. Binner and R. Moreno, "Wet forming of concentrated nano  
50  
51 BaTiO<sub>3</sub> suspensions," *J. Eur. Ceram. Soc.*, *In Press*.  
52  
53  
54 <sup>6</sup>F. F. Lange, "Powder Processing Science and Technology for increased Reliability," *J.*  
55  
56 *Am. Ceram. Soc.*, **72** [1] 3-15 (1989).  
57  
58  
59 <sup>7</sup>L. A. Wang and F. Aldinger, "Near Net Shape Forming of Advanced Ceramics," *Adv.*  
60  
*Eng. Mater.*, **3** [2] 110-13 (2000).

- 1  
2  
3  
4  
5  
6  
7  
8  
9  
10  
11  
12  
13  
14  
15  
16  
17  
18  
19  
20  
21  
22  
23  
24  
25  
26  
27  
28  
29  
30  
31  
32  
33  
34  
35  
36  
37  
38  
39  
40  
41  
42  
43  
44  
45  
46  
47  
48  
49  
50  
51  
52  
53  
54  
55  
56  
57  
58  
59  
60
- <sup>8</sup>I. Santacruz and J. Binner, “Rheological characterization and coagulation casting of Al<sub>2</sub>O<sub>3</sub>–nano zirconia suspensions,” *J. Am. Ceram. Soc., In Press*.
- <sup>9</sup>W. M. Sigmund, N. S. Bell and L. Bergström, “Novel Powder-Processing Methods for Advanced Ceramics,” *J. Am. Ceram. Soc.*, **83** [7] 1557-74 (2000).
- <sup>10</sup>I. Santacruz, M. I. Nieto and R. Moreno, “Alumina bodies with near-to-theoretical density by aqueous gelcasting using concentrated agarose solutions,” *Ceram. Int.*, **31** [3] 439-45 (2005).
- <sup>11</sup>J. A. Lewis, “Colloidal Processing of Ceramics,” *J. Am. Ceram. Soc.*, **83** [10] 2341-59 (2000).
- <sup>12</sup>H. B. Shan and Z. T. Zhang, “Slip Casting of Nanometre-Sized Tetragonal Zirconia Powder,” *Br. Ceram. Trans.*, **95** [1] 35-38 (1996).
- <sup>13</sup>L. P. Meier, L. Urech and L. J. Gauckler, “Tape casting of nanocrystalline ceria gadolinia powder,” *J. Eur. Ceram. Soc.*, **24** [15-16] 3753–58 (2004).
- <sup>14</sup>R. Moreno, “The role of slip additives in tape-casting technology: part I – solvents and dispersants,” *Am. Ceram. Soc. Bull.*, **71** [10] 1521-30 (1992).
- <sup>15</sup>J. Cesarano III and I. A. Aksay, “Stability of aqueous  $\alpha$ -Al<sub>2</sub>O<sub>3</sub> suspensions with poly(methacrylic acid) polyelectrolyte,” *J. Am. Ceram. Soc.*, **71** [4] 250-55 (1988).
- <sup>16</sup>R. Moreno Botella, (“Rheology of Ceramic Suspensions”) “Reología de Suspensiones Cerámicas,” Biblioteca de Ciencias, Published by Consejo Superior de Investigaciones Científicas, Madrid, Spain, 2005. (*In Spanish*).
- <sup>17</sup>D. R. Dinger, “Rheology for Ceramists,” Published by Dinger Ceramic Consulting Services, Clemson, USA, 2002.
- <sup>18</sup>G. Schramm, “A practical approach to Rheology and Rheometry,” Published by Thermo Electron (Karlsruhe) GmbH, Karlsruhe, Germany, 2004.

- 1  
2  
3  
4  
5  
6  
7  
8  
9  
10  
11  
12  
13  
14  
15  
16  
17  
18  
19  
20  
21  
22  
23  
24  
25  
26  
27  
28  
29  
30  
31  
32  
33  
34  
35  
36  
37  
38  
39  
40  
41  
42  
43  
44  
45  
46  
47  
48  
49  
50  
51  
52  
53  
54  
55  
56  
57  
58  
59  
60
- <sup>19</sup>J. Cesarano III and I. A. Aksay, "Processing of highly concentrated aqueous  $\alpha$ -alumina suspensions stabilized with polyelectrolytes," *J. Am. Ceram. Soc.*, **71** [12] 1062-67 (1988).
- <sup>20</sup>L.C. Guo, Y. Zhang, N. Uchida, K. Uematsu, "Adsorption effects on the rheological properties of aqueous alumina suspensions with polyelectrolyte," *J. Am. Ceram. Soc.*, **81** [3] 549-56 (1998).
- <sup>21</sup>E. P. Luther, J. A. Yanez, G. V. Franks, F. F. Lange, D. S. Pearson, "Effect of ammonium citrate on the rheology and particle packing of alumina slurries," *J. Am. Ceram. Soc.*, **78** [6] 1495-500 (1995).
- <sup>22</sup>P. C. Hidber, T. J. Graule, L. J. Gauckler, "Citric Acid-A dispersant for aqueous alumina suspensions," *J. Am. Ceram. Soc.*, **79** [7] 1857-67 (1996).
- <sup>23</sup>J. Davies and J. G. P. Binner, "The role of ammonium polyacrylate in dispersing concentrated alumina suspensions," *J. Eur. Ceram. Soc.*, **20** 1539-53 (2000).
- <sup>24</sup>J. Sun, L. Gao and J. Guo, "Influence of the initial pH on the adsorption behaviour of dispersant on nano zirconia powder," *J. Eur. Ceram. Soc.*, **19** 1725-30 (1999).
- <sup>25</sup>R. Moreno, A. Salomoni, and S. M. Castanho, "Colloidal filtration of silicon nitride aqueous slips. Part I: Optimization of the slip parameters," *J. Eur. Ceram. Soc.*, **18**, 405-416 (1998).
- <sup>26</sup>I. Santacruz, J. Binner, M. I. Nieto, R. Moreno, "Dispersion and rheology of aqueous suspensions of nanosized BaTiO<sub>3</sub>," *Submitted to J. Am. Ceram. Soc.*, August 2007.
- <sup>27</sup>F. Boschini, A. Rulmont, R. Cloots and R. Moreno, "Colloidal stability of aqueous suspensions of barium zirconate," *J. Eur. Ceram. Soc.*, **25** 3195-3201 (2005).
- <sup>28</sup>Z. Xie, J. Ma, Q. Xu, Y. Huang and Y. B. Cheng, "Effects of dispersants and soluble counter-ions on aqueous dispersibility of nano-sized zirconia powder", *Ceram. Int.*, **30** [2] 219-24 (2004).

1  
2  
3  
4  
5  
6  
7  
8  
9  
10  
11  
12  
13  
14  
15  
16  
17  
18  
19  
20  
21  
22  
23  
24  
25  
26  
27  
28  
29  
30  
31  
32  
33  
34  
35  
36  
37  
38  
39  
40  
41  
42  
43  
44  
45  
46  
47  
48  
49  
50  
51  
52  
53  
54  
55  
56  
57  
58  
59  
60

<sup>29</sup>J. G. P. Binner, B. Vaidhyanathan and A. Carney, "Microwave hybrid sintering of nanostructured YSZ ceramics," *Adv. Sci. Techn.*, **45** 835-844 (2006).

<sup>30</sup>M. Colic, G. Franks, M. Fisher and F. Lange, "Chemisorption of organofunctional silanes on silicon nitride for improved aqueous processing," *J. Am. Ceram. Soc.*, **81** [8] 2157-63 (1998).

<sup>31</sup>T. Fengqiu, H. Xiaoxian, Z. Yufeng and G. Jingkun, "Effect of dispersants on surface chemical properties of nano-zirconia suspensions," *Ceram. Int.*, **26** [1] 93-97 (2000).

<sup>32</sup>A. J. Sanchez-Herencia, C. Pascual, J. He, and F. F. Lange, "ZrO<sub>2</sub>/ZrO<sub>2</sub> Layered Composites for Crack Bifurcation," *J. Am. Ceram. Soc.*, **82** [6] 1512-18 (1999).

<sup>33</sup>A. R. Studart, E. Amstad, M. Antoni, L. J. Gauckler, "Rheology of concentrated suspensions containing weakly attractive alumina nanoparticles," *J. Am. Ceram. Soc.*, **89** [8] 2418-25 (2006).

<sup>34</sup>K. Lu, C. S. Kessler, R. M. Davis, "Optimization of a nanoparticle suspension for freeze casting," *J. Am. Ceram. Soc.*, **89** [8] 2459-65 (2006).

<sup>35</sup>O. Burgos-Montes, M. I. Nieto, R. Moreno, "Mullite compacts obtained by colloidal filtration of alumina powders dispersed in colloidal silica suspensions," *Ceram. Int.*, **33** [3] 327-3 (2007).

<sup>36</sup>J. G. P. Binner, I. Santacruz and K. Annapoorani, International patent application Publ. No. WO 2006/136780 A2, Publ. Date 28/12/06.

## Captions

- 1  
2  
3  
4  
5  
6  
7  
8  
9  
10  
11  
12  
13  
14  
15  
16  
17  
18  
19  
20  
21  
22  
23  
24  
25  
26  
27  
28  
29  
30  
31  
32  
33  
34  
35  
36  
37  
38  
39  
40  
41  
42  
43  
44  
45  
46  
47  
48  
49  
50  
51  
52  
53  
54  
55  
56  
57  
58  
59  
60
- Fig. 1. TEM images of the 3YSZ nanoparticles at different magnifications.
- Fig. 2. Evolution of the zeta potential as a function of pH for the diluted, 1.8 vol%, nanosuspension: without dispersant, with 2.5 wt% of Dispex A40, or TAC.
- Fig. 3. Evolution of the particle size and zeta potential as a function of pH with the addition of TMAH to 1.8 vol% nanosuspension.
- Fig. 4. Flow curves of dispersed suspensions containing 2.5 wt% Dispex A40 prepared with  $\text{NH}_4\text{OH}$  (17.0 vol% solids content) and TMAH (19.0 vol% solids content).
- Fig. 5. Flow curves of a 15.0 vol% suspension dispersed with Dispex A40 after 1 and 2 minutes of ultrasound. The basic agent was TMAH.
- Fig. 6. Effect of ultrasound time on the viscosity of a 19.0 vol% suspension dispersed with Dispex A40; a) flow curves and b) viscosity at  $100 \text{ s}^{-1}$  as a function of ultrasound exposure time. The basic agent was TMAH.
- Fig. 7. Effect of ageing on viscosity of a 16.0 vol% suspension with Dispex A40 subjected to different ultrasound exposure time. The basic agent was TMAH.
- Fig. 8. Average agglomerate size measured by laser scattering for Dispex based concentrated suspensions with and without ultrasound exposure.
- Fig. 9. FEG-SEM micrographs of the fracture surface of green bodies prepared from 15.0 vol% suspensions with TMAH and Dispex after a) 1 minute and b) 2 minutes of ultrasound, c) and d) green bodies from a dispersed 19.0 vol% suspension (TMAH & Dispex) subjected to 5 minutes of ultrasound, at different magnifications.

1  
2  
3  
4  
5  
6  
7  
8  
9  
10  
11  
12  
13  
14  
15  
16  
17  
18  
19  
20  
21  
22  
23  
24  
25  
26  
27  
28  
29  
30  
31  
32  
33  
34  
35  
36  
37  
38  
39  
40  
41  
42  
43  
44  
45  
46  
47  
48  
49  
50  
51  
52  
53  
54  
55  
56  
57  
58  
59  
60

Fig. 10. Viscosity vs. volume fraction curve for a suspension with TMAH and Dispex A40 using “multi-ultrasound”. Shear rate:  $100 \text{ s}^{-1}$ . Ultrasound application at 15.0, 19.0 and 28.0 vol%, the latter being the final solids content.

Fig. 11. Flow curves of suspensions with TMAH and TAC, a) without ultrasound, b) 24.0 vol% with different ultrasound times, c) 28.0 vol% without and with 2 min ultrasound at this solids loading, after 2 min ultrasound at 24.0 vol% (multi-ultrasound).

Fig. 12. Viscosity curves for the nanosuspensions: a) 24.0 vol% using TMAH & TAC after 6 min ultrasound, b) 19.0 vol% prepared using TMAH & Dispex A40 after multi-ultrasound, c) 28.0 vol% using TMAH & TAC after multi-ultrasound treatments.

Fig. 13. FEG-SEM micrographs of sintered samples prepared from a 19.0 vol% suspension with TMAH & Dispex with soaking times of: a) 5 h, b) 10 h; c) a green sample prepared from a 28.0 vol% suspension with TMAH & TAC after multi-ultrasound and d) the sample in (c) after sintering (soaking time: 10 h).

Table I. Summary of the characteristics of the nanosuspensions prepared under a range of different conditions.

Dispersant	Dispersant content / wt%	Solids loading / vol%	Basic agent	Ultrasound / min	Viscosity / mPa s at 100 s <sup>-1</sup>	pH ± 0.1	
-	0	5.0	-	0	2	2.4	
PEI	2.0	5.0	-	0	10	4.6	
Dispex A40	2.5	17	Ammonia	0	1000	9.5	
		19	TMAH	2	300		
				6	45		
		28		Multiultrasound	700		
TAC	2.5	24	TMAH	0	1400	9.5	
		28		Multiultrasound	2		75
					6		15
		2		320			

Table I.

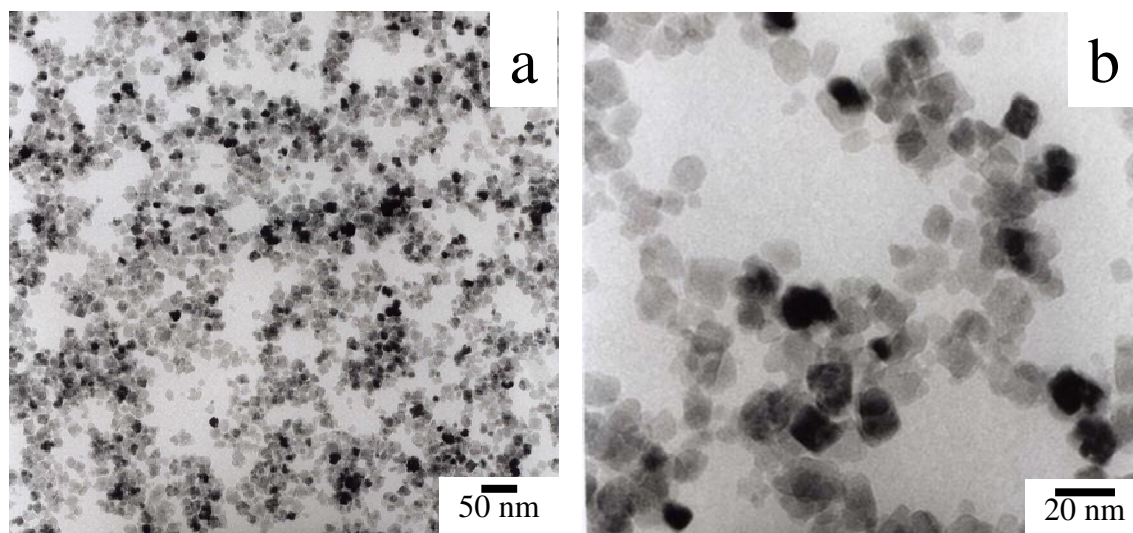


Fig. 1



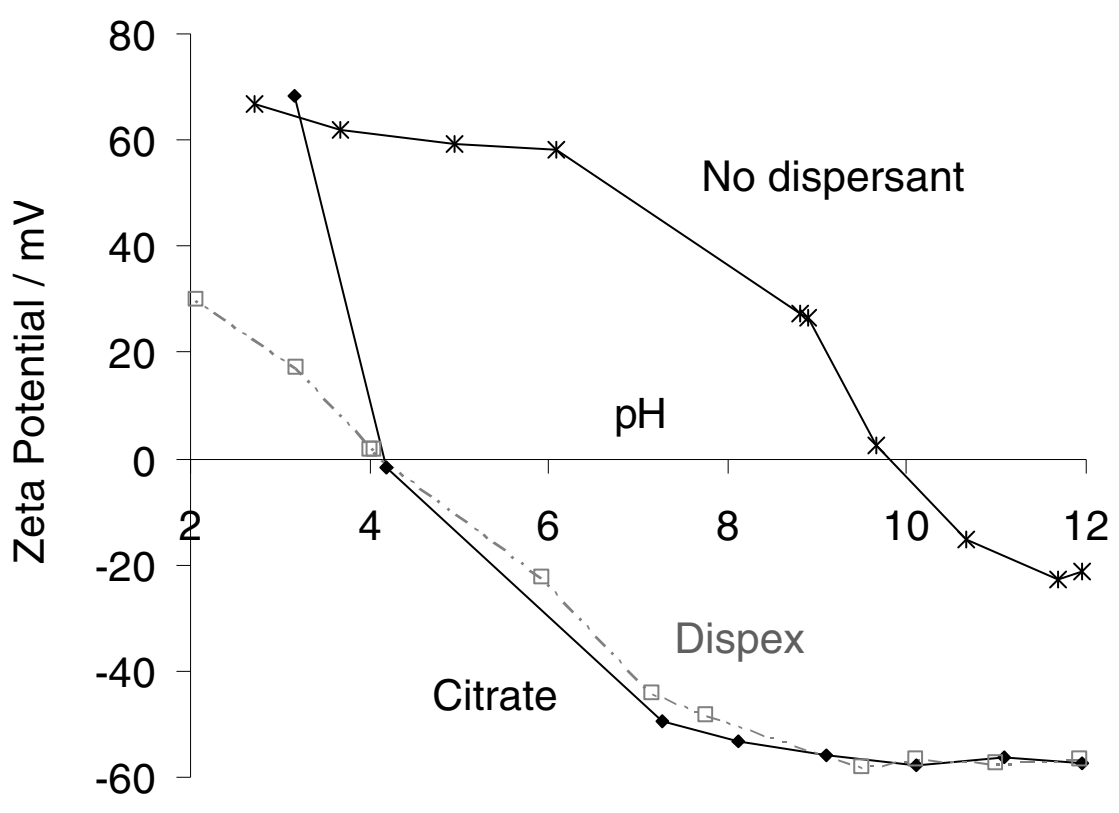


Fig. 2

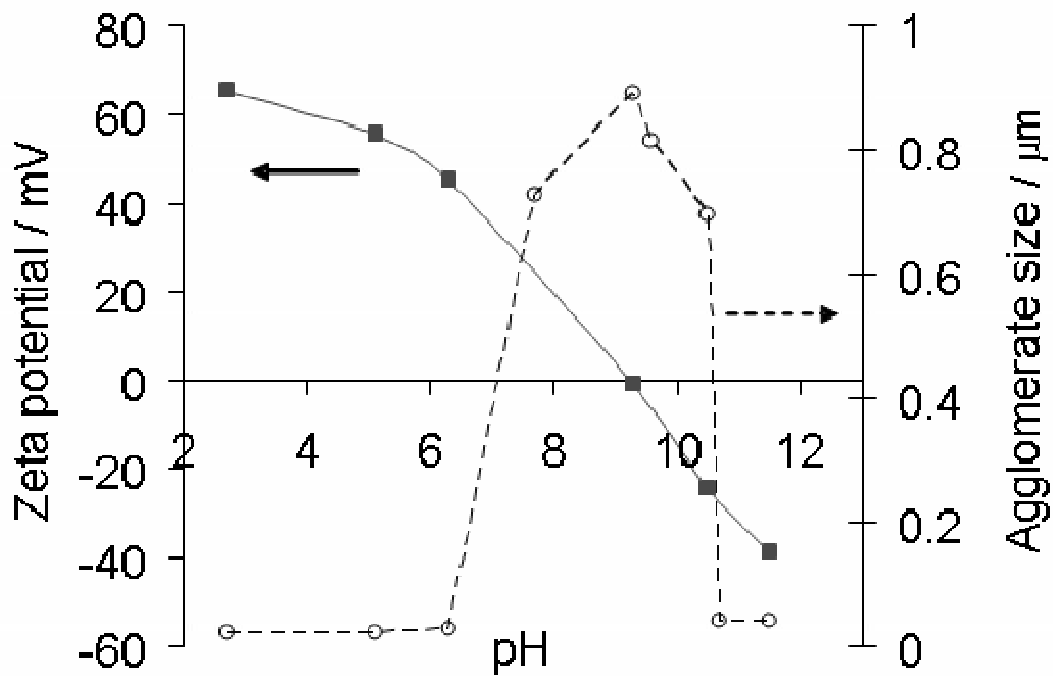


Fig 3

1  
2  
3  
4  
5  
6  
7  
8  
9  
10  
11  
12  
13  
14  
15  
16  
17  
18  
19  
20  
21  
22  
23  
24  
25  
26  
27  
28  
29  
30  
31  
32  
33  
34  
35  
36  
37  
38  
39  
40  
41  
42  
43  
44  
45  
46  
47  
48  
49  
50  
51  
52  
53  
54  
55  
56  
57  
58  
59  
60

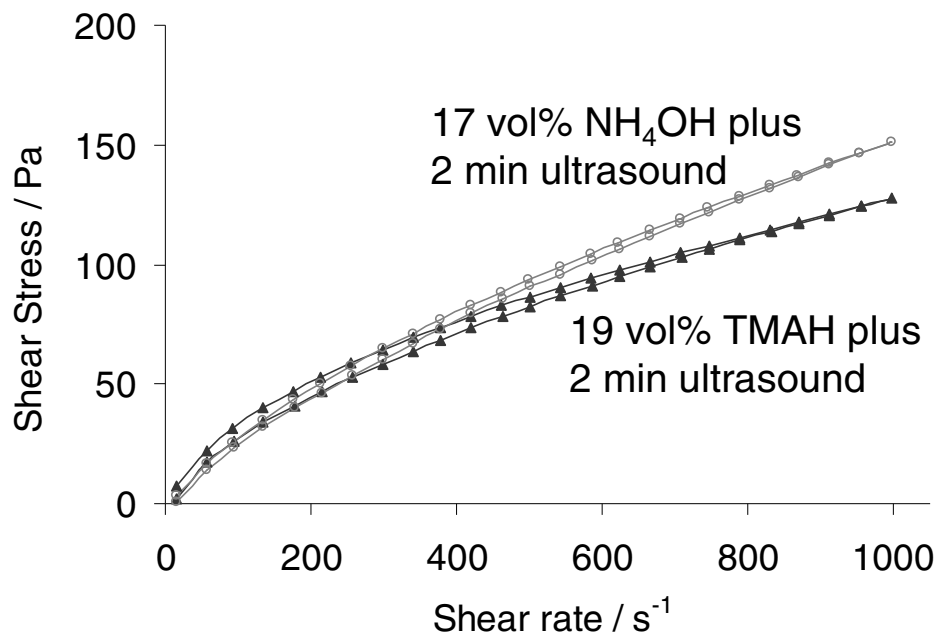


Fig 4

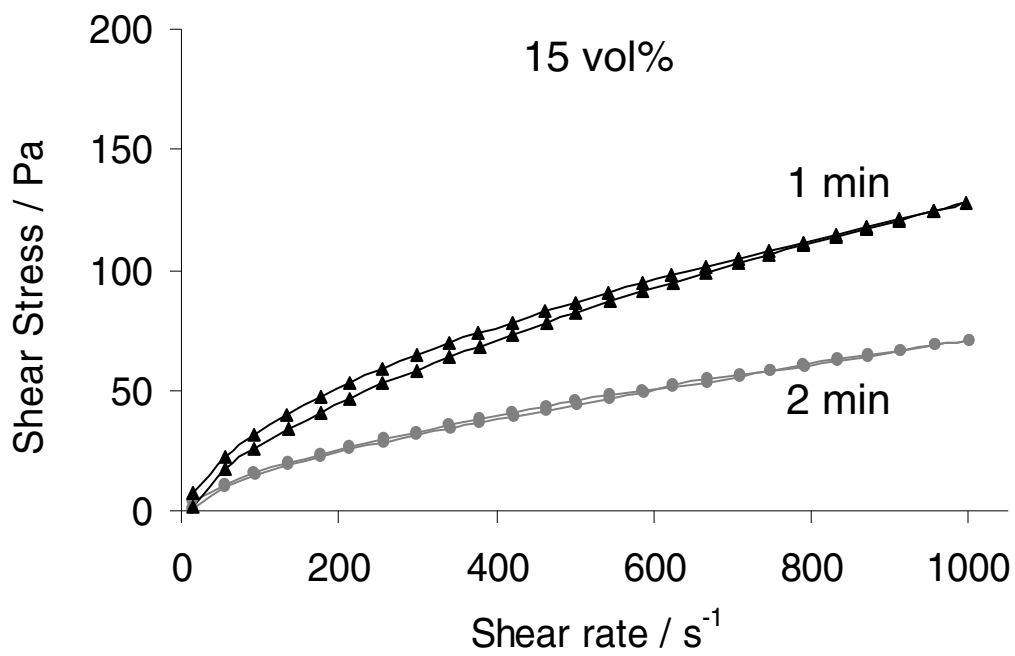


Fig 5

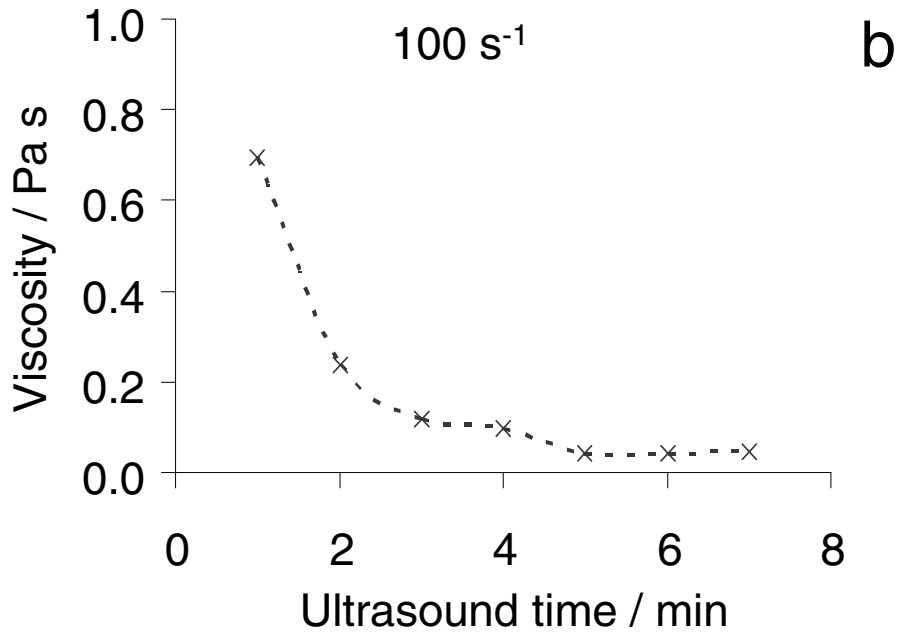
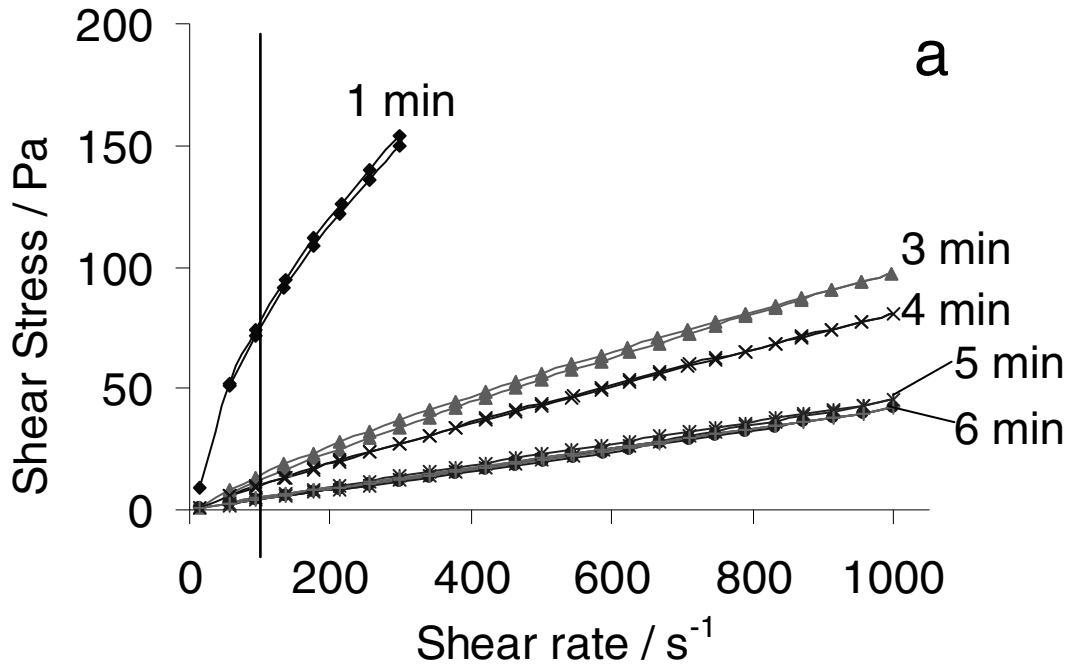


Fig 6

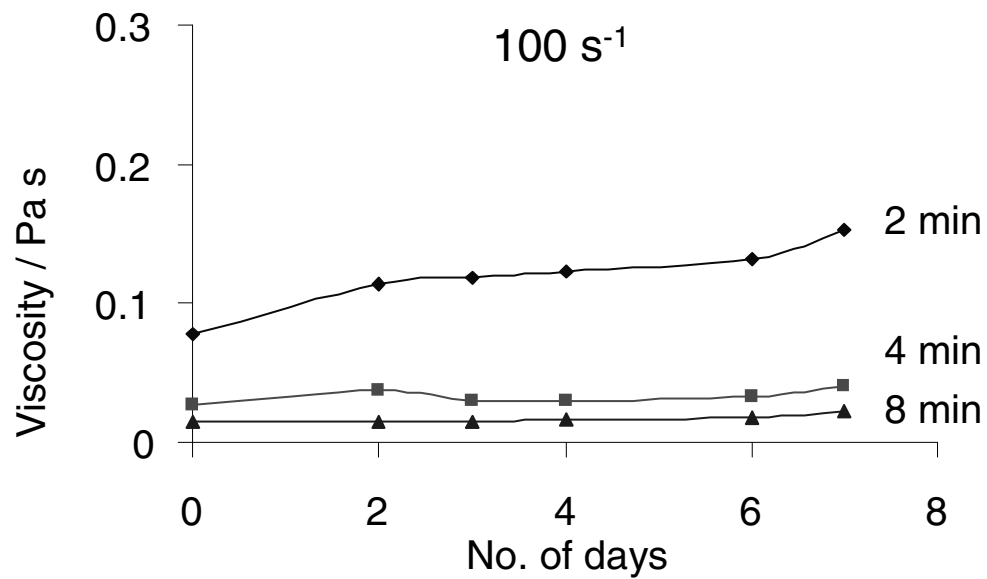


Fig 7

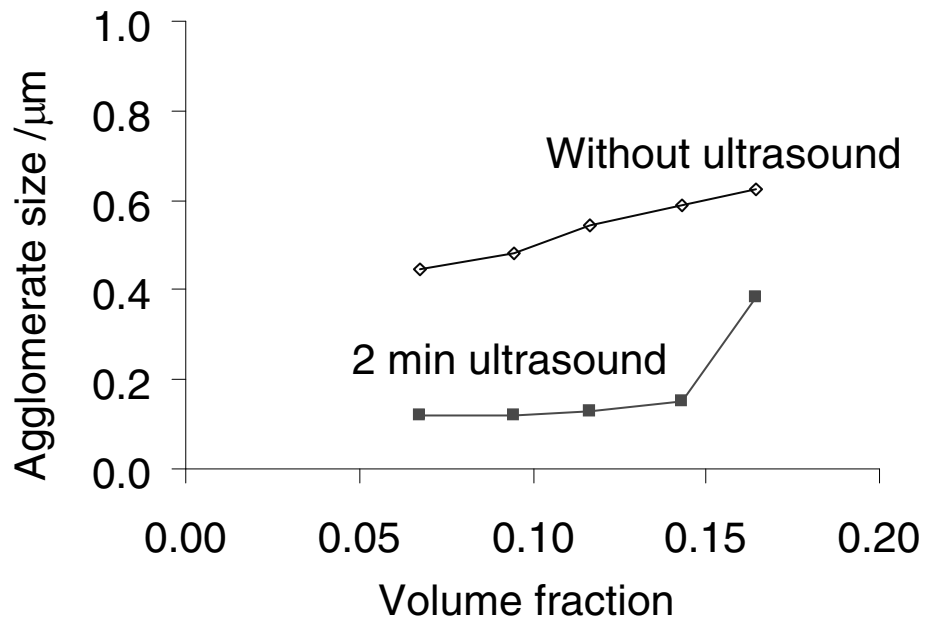


Fig 8

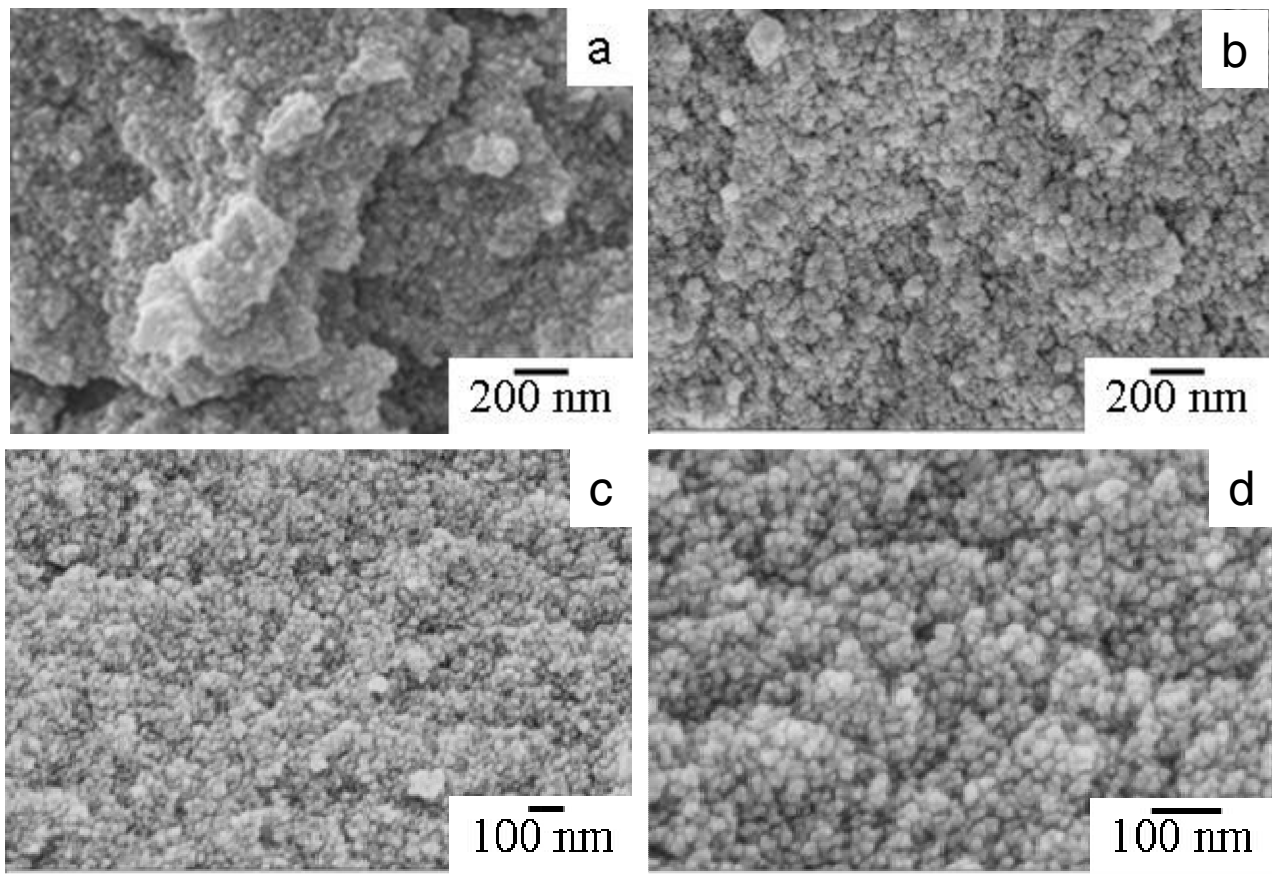


Fig 9



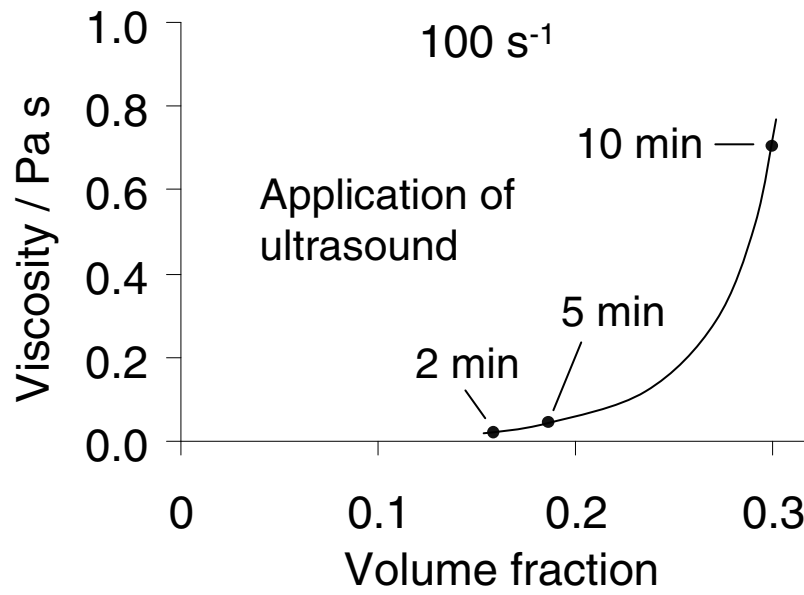


Fig 10

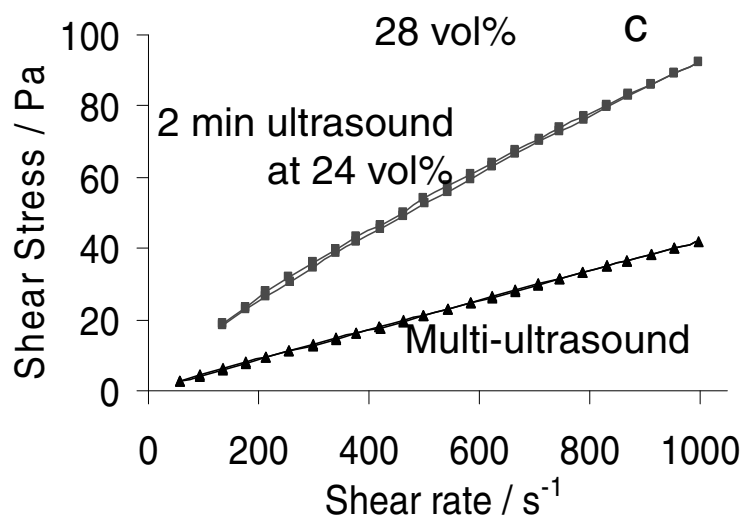
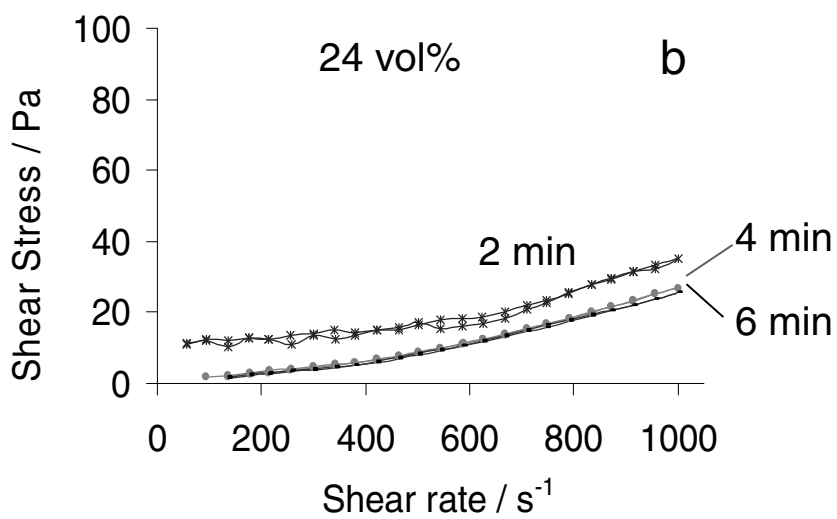
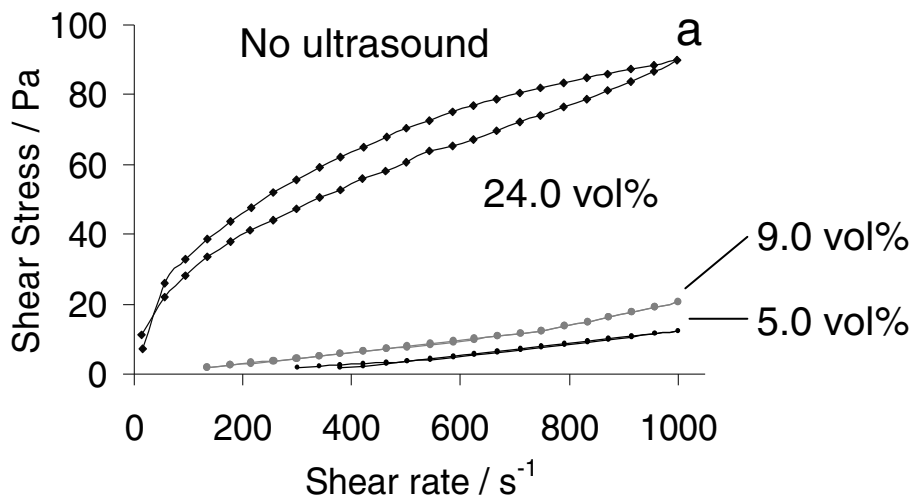


Fig 11

1  
2  
3  
4  
5  
6  
7  
8  
9  
10  
11  
12  
13  
14  
15  
16  
17  
18  
19  
20  
21  
22  
23  
24  
25  
26  
27  
28  
29  
30  
31  
32  
33  
34  
35  
36  
37  
38  
39  
40  
41  
42  
43  
44  
45  
46  
47  
48  
49  
50  
51  
52  
53  
54  
55  
56  
57  
58  
59  
60

1  
2  
3  
4  
5  
6  
7  
8  
9  
10  
11  
12  
13  
14  
15  
16  
17  
18  
19  
20  
21  
22  
23  
24  
25  
26  
27  
28  
29  
30  
31  
32  
33  
34  
35  
36  
37  
38  
39  
40  
41  
42  
43  
44  
45  
46  
47  
48  
49  
50  
51  
52  
53  
54  
55  
56  
57  
58  
59  
60

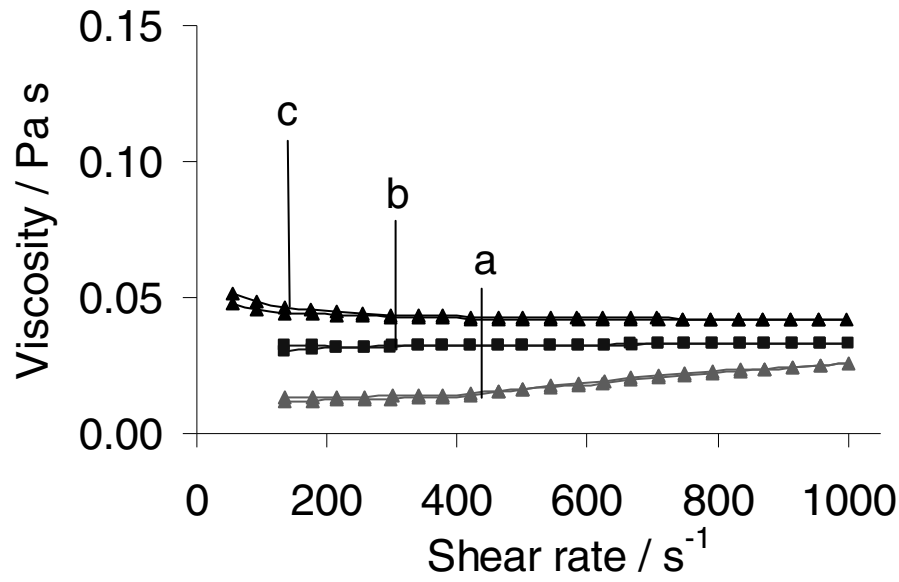


Fig 12

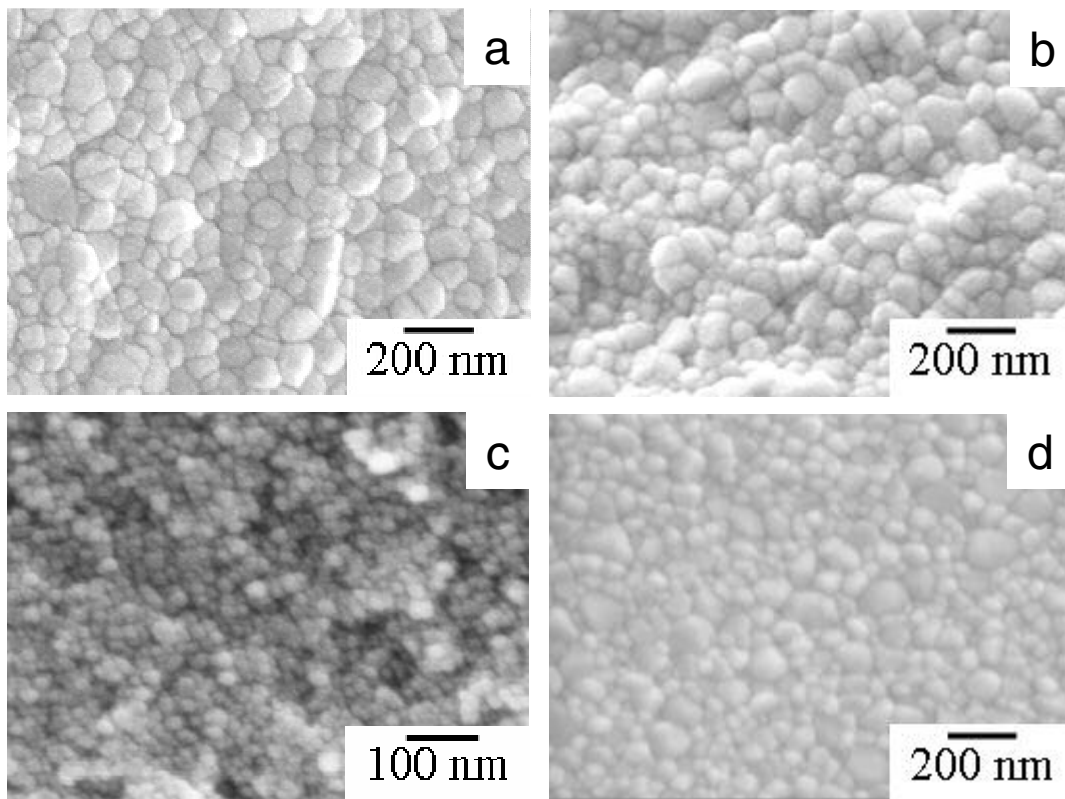


Fig 13